Absence of Evidence for Metabolite-Modulated Association between α-Glycerol-3-phosphate Dehydrogenase and L-Lactate Dehydrogenase†

Eric A. Lehoux,* Sharon M. Baker,‡ Marina V. Kovina, Franklin A. Hays,§ and H. Olin Spivey

Department of Biochemistry and Molecular Biology, Noble Research Center, Oklahoma State University, Stillwater, Oklahoma 74078

Received November 26, 2002; Revised Manuscript Received March 21, 2003

ABSTRACT: Evidence for the NADH-modulated formation of a complex between α-glycerol-3-phosphate dehydrogenase and L-lactate dehydrogenase was reported [Yong, H., Thomas, G. A., and Peticolas, W. L. (1993) *Biochemistry 32*, 11124−11131]. This NADH-modulated association suggested a mechanism of potentially great importance to enzyme modulation and the controversial phenomena of direct NADH channeling. In the present paper, we reproduce with additional controls the experiments described by Yong et al. ((1993) *Biochemistry 32*, 11124−11131). Our results conclusively demonstrate the absence of detectable association between α-glycol-3-phosphate dehydrogenase and L-lactate dehydrogenase.

Evidence for the metabolite-modulated formation of an equilibrium complex between α-glycerol-3-phosphate dehydrogenase (αGDH; EC 1.1.1.8)[1] and L-lactate dehydrogenase (LDH; EC 1.1.1.27) was reported (*1*). Previous attempts to detect a complex between these two dehydrogenases were unsuccessful (*2*, *3*). However, Yong et al. (*1*) reported detecting a strong complex ($K_a = 2.0 \pm 0.6\ \mu M^{-1}$) in the presence of a very limited substoichiometric [NADH], a condition not tested in previous studies. The detection of a weak complex ($K_a = 0.04 \pm 0.02\ \mu M^{-1}$) in the absence of NADH, but not in the presence of a saturating [NADH], was also reported (*1*). This NADH-modulated association suggested an unprecedented but reasonable mechanism of enzyme interactions of potentially great importance to enzyme modulation and the controversial phenomena of direct NADH transfer (channeling) between dehydrogenases (for review, ref *4*).

Using several methods, we recently attempted to detect association between dehydrogenases reported, like the αGDH−LDH pair, to channel NADH directly (*5*). Failure to detect association, even in the presence of substoichiometric concentrations of NADH, prompted us to revisit the study of Yong et al. (*1*). In the present paper, we describe modified Hummel−Dreyer chromatography experiments reproducing this study with additional controls. Our results conclusively demonstrate the absence of detectable NADH-modulated association between αGDH and LDH.

EXPERIMENTAL PROCEDURES

Materials. The TSK-GEL G3000SWXL high performance liquid chromatography column (7.8 mm i.d. × 30 cm length; 32 160 theoretical plates, as determined by the supplier) and the TSK-GEL SWXL guard columns (6 mm i.d. × 4 cm length) were purchased from TosoHaas. αGDH from rabbit muscle was purchased from Sigma Chemical Co. (catalog no. G-6751), ICN (catalog no. 104 938, discontinued), and Boehringer Mannheim (catalog no. 127 779). LDH from porcine heart was purchased from ICN (catalog no. 151 532). Alcohol dehydrogenase from equine liver (ADH, EC 1.1.1.1; catalog no. 102 741) was purchased from Boehringer Mannheim. Disodium β-NADH (catalog no. N-8129) and glucose-6-phosphate dehydrogenase from *Leuconostoc mesenteroides* (G6PDH; EC 1.1.1.49) were purchased from Sigma Chemical Co. FC-43 oil (3M Company) was purchased from Beckman Coulter. All other reagents were purchased from Sigma Chemical Co., Fluka Chemical Co., or Fisher Scientific. Chromatography was performed with a ÄKTA explorer liquid chromatography system from Pharmacia Biotech equipped with a 10 mm path length and 8 μL UV flow cell.

Enzyme Preparation and Assays. Prior to all measurements, untreated enzymes were dialyzed for ca. 6 h at 4 °C against MOPS buffer (50 mM MOPS, pH 6.9 at room temperature, 100 mM NaCl, 0.5 mM EDTA, 0.5 mM dithiothreitol, and 0.02% (w/v) NaN_3). The enzyme dialysates were clarified by centrifugation at 16 000*g* for 15 min at 4 °C and used without delay. All injected samples contained less than 100 μM $(NH_4)_2SO_4$ as determined with modern Nessler reagent (*6*). The [ADH], [αGDH], and [LDH] were determined spectrophotometrically as described by Yong et al. (*1*). The M_r values of these proteins are 79 000, 78 000, and 144 000, respectively. [NADH] was determined enzymatically under the assay conditions of αGDH (below)

† This research was supported under OAES Project OKLO-1393, National Science Foundation Award MCB-9513613, and Oklahoma Center for the Advancement of Science and Technology (OCAST) Award HR98-061 to H.O.S. E.A.L. was a recipient of a FCAR scholarship from Québec (Canada). F.A.H. was a recipient of a scholarship from an undergraduate education grant from the Howard Hughes Medical Institute to Oklahoma State University.

* Corresponding author. E-mail: elehoux@biochem.okstate.edu.

‡ Present address: Department of Physiological Sciences, Oklahoma State University, Stillwater, OK 74078.

§ Present address: Department of Biochemistry and Biophysics, Oregon State University, Corvallis, OR 97331.

[1] Abbreviations: ADH, alcohol dehydrogenase; αGDH, α-glycerol-3-phosphate dehydrogenase; G6P, glucose 6-phosphate; G6PDH, glucose-6-phosphate dehydrogenase; LDH, L-lactate dehydrogenase.

10.1021/bi027244b CCC: $25.00
Published on Web 05/03/2003

except that excess αGDH and ca. 100 μM NADH were used. The molar absorbtivity at 340 nm of αGDH-bound NADH was determined using a partitioned cuvette (Precision Cells, Inc., catalog no. PK100).

The enzymes were assayed essentially as described by Bergmeyer (ref *7*; αGDH) and Bergmeyer (ref *8*; ADH and LDH). All assays were performed at 25 ± 0.5 °C. The specific activities of the dialyzed αGDH, ADH, and LDH were 410 ± 30 (n = 4), 3.30 ± 0.30 (n = 2), and 360 ± 30 units per mg protein (n = 4), respectively. One unit of enzyme activity is defined as the quantity of enzyme that transforms 1 μmol of substrate per min under the specified assay conditions. The 280 nm/260 nm absorbance ratio of dialyzed ADH (1.46 ± 0.01, n = 6), LDH (2.01 ± 0.01, n = 6), and αGDH (1.55 ± 0.01, n = 8 and 1.60 ± 0.01, n = 6, before and after treatment with activated charcoal, respectively) indicate that the untreated enzymes were free or near free of bound nucleotides.

Modified Hummel−Dreyer Chromatography. A guard column was connected between the pump and the injection loop of the chromatography system to prevent loss of resolution while protecting the main column from the protein in the column equilibration buffer. The gel filtration column was equilibrated with MOPS buffer containing NADH and αGDH or ADH at the indicated concentrations, 2 mM glucose 6-phosphate (G6P), and 2 μg/mL G6PDH (ca. 650 U/mg). These last two components were included in the buffer to maintain the [NADH] constant (see ref *9*). The very low [G6PDH] used precluded its contribution to changes in recorded absorbances. The injected samples (100 μL) were pumped through the column at a flow rate of 0.4 mL/min. Samples contained a fixed concentration of LDH (0 or 1.65 μM) and varying concentrations of αGDH or ADH in MOPS buffer containing NADH, G6PDH, and G6P, as above. Absorbance was monitored continuously at 280 and 340 nm. Chromatography was performed in a cold room (ca. 4 °C) with the column equilibration buffer kept on ice. The temperature of the effluent at the exit of the column was ca. 8.0 °C.

Analytical Ultracentrifugation. Sedimentation equilibrium data were collected with a Beckman Optima XL-A analytical ultracentrifuge using a four-hole An-60Ti rotor, double-sector charcoal-filled Epon centerpieces of 3 mm optical path length, and quartz windows. The experiments were performed at 8 °C with three cells containing 27.8 μM αGDH, 13.9 μM LDH, and a mixture of the two enzymes at the same concentrations. The enzymes were prepared in MOPS buffer containing 13.9 μM NADH, 2 mM G6P, and 2 μg/mL G6PDH. The reference sectors contained this solution without αGDH and LDH. FC-43 oil (4 μL) was placed at the bottom of the sample sectors to minimize light reflection. Rotor speeds of 11 000 and 16 000 rpm were used. Equilibrium was verified by a random distribution of residuals. Radial scans were performed at 280 nm. High-speed (42 000 rpm) sedimentation was performed to determine the experimental baseline.

Data Presentation and Analysis. Unless otherwise specified, all data are reported as means ± SD. Untransformed original data are presented. Enzyme concentrations are expressed in terms of native enzymes. Since native αGDH and ADH are homodimers, and native LDH is a homotetramer, the [NADH]/[enzyme subunits or NADH binding sites] ratios are 0.5, 0.5, and 0.25 of the [NADH]/[native enzyme] ratios for αGDH, ADH, and LDH, respectively.

The chromatographic elution profiles were analyzed using UNICORN software version 2.30 (Pharmacia Biotech). A lowest and highest probable horizontal baseline was user-defined for each elution profile, and a K_a corresponding to each baseline was calculated as described by Yong et al. (*1*) for each series of elution profiles. The K_a values presented are the average of these two K_a values. The plots of integrated peak areas versus [αGDH] or [ADH] are available as Supporting Information.

The slight differences between the nominal [αGDH] or [ADH] in the column and the nominal concentration of injected αGDH or ADH needed to produce a flat baseline in the elution profiles collected at 280 nm in the absence of LDH were determined for each series of profiles. These differences were used to correct the [αGDH] or [ADH] in the column as described by Yong et al. (*1*). The [NADH] in the column was not corrected because the corresponding differences were negligible.

The sedimentation equilibrium data was analyzed using UltraScan software version 6.0 (*10*) running under SuSE 8.1 distribution of the Linux operating system, and Beckman sedimentation equilibrium software version 3.01. Simulated data was generated using computer programs written by H. O. Spivey. The partial specific volumes of αGDH (0.7473 cm^3/g) and LDH (0.7490 cm^3/g) were calculated using the computer program SEDNTERP (developed by D. B. Haynes, T. Laue, and J. Philo; http://www.bbri.org/RASMB/rasmb.html).

RESULTS AND DISCUSSION

Principle of the Modified Hummel−Dreyer Chromatography of LDH and αGDH. LDH, αGDH, and NADH are injected onto a gel filtration column equilibrated with αGDH and NADH (see legend of Figure 1). In the absence of complex formation between LDH and αGDH, a flat baseline (i.e., the absence of a peak or trough) is expected at the retention time of injected αGDH when the [αGDH] in the injected sample is equal to the [αGDH] in the column. However, in the presence of detectable association, αGDH is expected to elute more rapidly as part of a αGDH−LDH complex than αGDH alone, thereby causing a trough at the retention time of injected αGDH (a complex peak eluting more rapidly than LDH may or may not be observed depending on the K_a of the complex). Therefore, in the presence of association, the [αGDH] in the injected sample required to produce a flat baseline at the retention time of injected αGDH will need to be higher than the [αGDH] in the column because additional αGDH will be needed to fill the trough of injected αGDH caused by complex formation. The K_a for the αGDH−LDH complex is determined from the difference between the [αGDH] needed in the injected sample to produce a flat baseline in the absence and presence of LDH (see Experimental Procedures).

Results of the Modified Hummel−Dreyer Chromatography of LDH and αGDH. The elution profiles we present were recorded at 280 and 340 nm to monitor [protein] and [NADH], respectively. The elution profiles recorded at 280 nm reproduce the data of Yong et al. (*1*), whereas the profiles recorded at 340 nm provide critical new information. In Figure 1A, we present a series of chromatographic elution

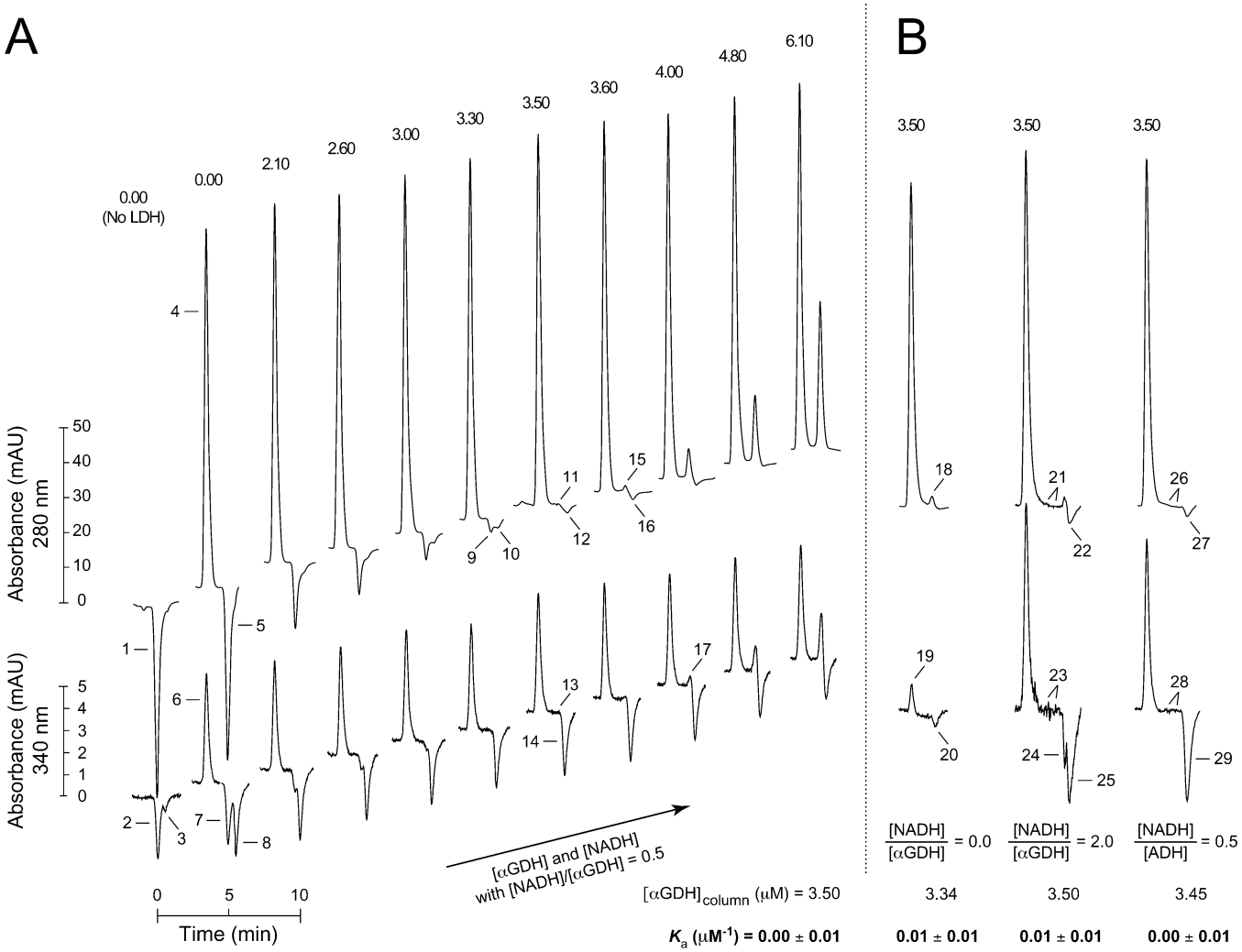

FIGURE 1: Elution profiles from the modified Hummel−Dreyer chromatography of LDH and αGDH and of LDH and ADH. (A) Series of elution profiles of LDH and αGDH collected at [NADH]/[αGDH] = 0.5. The column was equilibrated with 3.50 μM of αGDH. The [LDH] in the injected samples was 1.65 μM unless otherwise indicated. The [αGDH] in the injected samples was 0.00, 2.10, 2.60, 3.00, 3.30, 3.50, 3.60, 4.00, 4.80, and 6.10 μM as indicated above each profile. (B) Selected elution profiles of LDH and αGDH collected at [NADH]/[αGDH] = 0 and 2.0 and of LDH and ADH collected at [NADH]/[ADH] = 0.5. The column was equilibrated with 3.34 and 3.50 μM of αGDH at [NADH]/[αGDH] = 0 and 2.0, respectively, and 3.45 μM of ADH at [NADH]/[ADH] = 0.5. The [LDH] and [αGDH] in the injected samples were 1.65 and 3.50 μM, respectively. The time and absorbance scales apply to both panel A and panel B. Note the 10-fold difference between the scales of absorbance at 280 and 340 nm. K_a values were calculated as described under Experimental Procedures. Peak/through assignments for panels A and B: 1, 2, 5, 7, and 9, troughs of apo- and holo-αGDH; 3, 8, 10, 12, 14, 16, 20, and 24, troughs of αGDH-bound NADH with a small contribution from free NADH (trough 20 is due to the presence of traces of αGDH-bound NADH in the enzyme preparation); 4 and 6, peaks of apo- and holo-LDH; 11 and 13, flat baselines at the retention time of injected αGDH; 15 and 17, peaks of apo- and holo-αGDH; 18, peak of apo-αGDH; 19, peak of apo-LDH; 21, 23, 26, and 28, flat baselines at both the retention time of injected αGDH or ADH and the position of troughs 12 and 14; 22, trough of free NADH with a small contribution from αGDH-bound NADH; 25, 27, and 29, troughs of free NADH. For more details, see Results and Discussion. Typical elution profiles are shown.

profiles of LDH and αGDH collected at [NADH]/[αGDH] = 0.5. Key elution profiles of LDH and αGDH collected at [NADH]/[αGDH] = 0 and 2.0, and of LDH and ADH collected at [NADH]/[ADH] = 0.5 (a negative control), are presented in Figure 1B. These key profiles were selected from series of elution profiles available as Supporting Information. The K_a values determined from these profiles are presented in Figure 1.

Interpretation of the Results. At [NADH]/[αGDH] = 0.5, when the [αGDH] in the injected sample was equal to the [αGDH] in the equilibrated column, a flat baseline (Figure 1A, baseline 11) was obtained at the retention time of injected αGDH. For reasons discussed above, this indicates a lack of detectable association between LDH and αGDH (K_a = 0.00 ± 0.01 μM^{-1}). However, a small trough (Figure 1A, e.g., trough 12) was observed eluting 1 min 8 s ± 2 s (n = 4) later than injected αGDH. It is the mistaken identification of this trough as injected αGDH that led Yong et al. (*1*) to erroneously interpret their results as evidence of complex formation between αGDH and LDH.

To understand the correct origin of this trough (Figure 1A, e.g., trough 12), we will consider first the simple situation where αGDH, and thereby NADH, are omitted from the injected sample (Figure 1A, second profiles from the left, and Figure 2). As illustrated in Figure 2, after the injection of apo-LDH in buffer, the following events occur: (1) Apo-LDH migrates ahead of the injected buffer where it encounters and binds free NADH (in competition with αGDH). This greatly enlarges the band of buffer devoid of free NADH (to visualize the relative contribution to this band of the

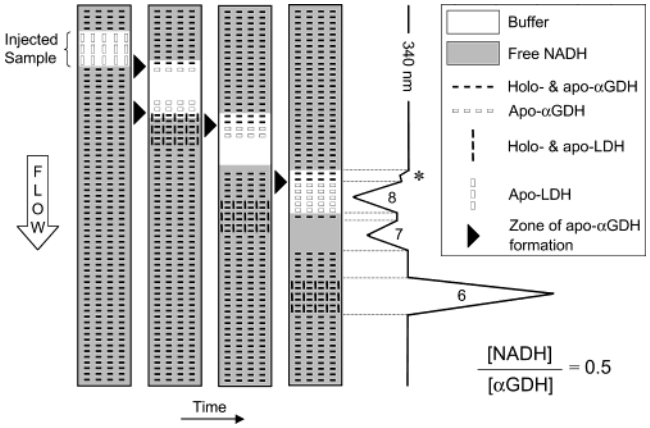

FIGURE 2: Diagram of the modified Hummel−Dreyer chromatography of LDH and αGDH at [NADH]/[αGDH] = 0.5 for the injected sample containing LDH but no αGDH and NADH. The elution profile represents absorbance measured at 340 nm. The peak labels refer to Figure 1A. The asterisk identifies a trough of free NADH that is barely visible at [NADH]/[αGDH] = 0.5 (Figure 1A) but clearly visible at [NADH]/[αGDH] = 2.0 (Figure 1B, trough 25).

binding of free NADH by apo-LDH and the omission of NADH from the injected sample, compare the size of troughs 8 and 3 in Figure 1A). (2) The apo- and holo-αGDH (in the column equilibration buffer) pumped into the column, *after the injection of the sample*, migrates into this enlarged band of NADH-deficient buffer. (3) As the holo form of this αGDH moves into NADH-deficient buffer, it releases its bound NADH (i.e., forms apo-αGDH). The newly formed apo-αGDH absorbs less at 340 nm than the corresponding holo-αGDH with which the column was equilibrated. This explains trough 8 in Figure 1A: it is due to a deficit of αGDH-bound NADH. Trough 14 in Figure 1A, and the other troughs in this series, are similarly explained (note that because of the presence of LDH the [NADH]/[dehydrogenase] in the injected samples is considerably lower than in the equilibrated column). As shown in Figure 1A, the elution time of troughs 14 (A_{340nm}) and 12 (A_{280nm}) coincide precisely. Furthermore, the ratio of the area of trough 12 over that of trough 14 (1.1 ± 0.1, $n = 6$) is identical, within experimental error, to the A_{280nm}/A_{340nm} ratio of αGDH-bound NADH (1.02 ± 0.07; estimated from the A_{280nm}/A_{340nm} ratio of free NADH, 0.62 ± 0.04, $n = 6$ and the ratio of A_{340nm} of αGDH-bound NADH/$A_{340\ nm}$ of free NADH, 0.61 ± 0.06, $n = 3$). This indicates that trough 12 is due to the presence of trough 14 (i.e., to a deficit of αGDH-bound NADH) and not to an accelerated elution of αGDH caused by complex formation with LDH.

Additional Chromatographic Evidence in Support of our Interpretation. The assignment of trough 12 and similar troughs (Figure 1A) to a deficit of αGDH-bound NADH explains the apparent displacement of the peak of injected αGDH (Figure 1A, e.g., peak 15) toward a shorter retention time by the overlap of this peak with a neighboring trough (e.g., trough 16). This overlap also explains the anomalously high [αGDH] needed in the injected sample to produce a flat baseline at the retention time of trough 12.

Our results also offer a simple explanation for the reported NADH modulation and the results obtained with ADH (a negative control). At [NADH]/[αGDH] = 0 (Figure 1B), the absence of a trough corresponding to trough 12 in Figure 1A is explained by the absence of holo-αGDH in the equilibrated column. As noted in the introductory paragraphs, Yong et al. (*1*) reported detecting weak association (near the detection limit) between αGDH and LDH in the absence of NADH. However, our inability to reproduce this result ($K_a = 0.01 \pm 0.01\ \mu M^{-1}$ in our study vs $0.04 \pm 0.02\ \mu M^{-1}$ in ref *1*), together with the failure of recent studies to detect association using tryptophan phosphorescence lifetime measurements (*11*) and agarose electrophoresis (*5*), leads us to conclude that there is no detectable association between αGDH and LDH at [NADH]/[αGDH] = 0.

At [NADH]/[αGDH] = 2 (Figure 1B), the NADH-deficient area created by LDH binding free NADH is considerably smaller than at [NADH]/[αGDH] = 0.5 because of the much higher [free NADH]. As a result, the troughs of αGDH-bound NADH corresponding to troughs 12 and 14 in Figure 1A are smaller and displaced to a later elution time (Figure 1B, troughs 22 and 24). In fact, the presence of troughs 24 and 25 (Figure 1B) indicates that trough 22 is comprised of two unresolved troughs: a trough of αGDH-bound NADH and a comparatively large trough of free NADH at the retention time of injected free NADH—a trough of free NADH was barely visible at [NADH]/[αGDH] = 0.5 because of the negligible [free NADH].

Finally, Yong et al. (*1*) replaced αGDH with ADH as a negative control for association. ADH and αGDH have a similar M_r and because of chiral specificity considerations (*12*), ADH is not expected to channel NADH directly to LDH or to form a complex with this enzyme. This negative control appeared to support the conclusions of Yong et al. (*1*). However, the presence of troughs 27 and 29 (Figure 1B) at the retention time of injected free NADH indicates that at [NADH]/[ADH] = 0.5, unlike at [NADH]/[αGDH] = 0.5, most of the total NADH was free (the NADH binding capacity of ADH was ca. 10-fold lower than that of αGDH presumably because of the presence of non-native NADH binding sites; see ref *9*). This explains the absence of a trough of ADH-bound NADH (Figure 1B, baseline 26) similar to trough 12 in Figure 1A.

Confirmation of the Absence of Detectable Association between αGDH and LDH by Analytical Ultracentrifugation. Sedimentation equilibrium experiments were performed to search for the presence of a complex between αGDH and LDH at [NADH]/[αGDH] = 0.5. The data collected from single-species samples of αGDH and LDH were fit to a single ideal component model. The M_w values calculated from this fit are $81\,800 \pm 1\,300$ and $141\,000 \pm 2\,000$ for αGDH and LDH, respectively. These values are in good agreement with the single species M_r values of αGDH (78 000) and LDH (144 000). The data collected from a sample containing a mixture of αGDH and LDH were fit to an ideal two-component noninteracting model. The M_w values calculated from this fit ($80\,500 \pm 3\,000$ and $147\,000 \pm 15\,000$) are similar to the M_w values calculated from the fit of the single-species samples (above). This indicates an absence of detectable association between αGDH and LDH. To quantify the minimum detectable level of association in our experiments, the profiles of the two-enzyme mixture were compared with a set of simulated profiles (generated using sedimentation parameters from the analysis of the individual enzymes) representing different levels of association between two ideal components. This comparison established an upper

limit of 0.01 μM^{-1} for the K_a of a complex between αGDH and LDH at [NADH]/[αGDH] = 0.5. This value is in excellent agreement with the results of our modified Hummel−Dreyer chromatography study.

Conclusion. Our study clearly demonstrates the absence of detectable NADH-modulated association between αGDH and LDH. Since direct NADH channeling requires at least a transient interaction between the channeling dehydrogenases, previous studies interpreted an absence of detectable association between αGDH and LDH as evidence against this phenomenon (*2*, *3*). However, it is not conclusive evidence. As recently emphasized, enzymes with protein substrates can catalyze reactions efficiently without detectable association (*13*). In addition, using simple and rigorous enzyme kinetic theory, we have recently shown that it is possible for direct NADH channeling to proceed without a detectable enzyme−enzyme complex (manuscript in preparation). Therefore, the absence of direct physical evidence of a complex between dehydrogenases reported to channel NADH directly does not negate direct NADH channeling. However, it signifies that the evidence in support of direct NADH-channeling now rests solely on steady-state kinetic data collected using the enzyme buffering method.

ACKNOWLEDGMENT

The authors gratefully acknowledge Dr. Zeljko Svedruzic for helpful suggestions, Brandi N. Simmons, Eldon C. Wagner, and Phillip P. Smith for excellent technical assistance, the Recombinant DNA/Protein Resource Facility at Oklahoma State University for the use of the ÄKTA explorer liquid chromatography system, and the Oklahoma State University Center for Analytical Ultracentrifugation for the use of the Beckman Optima XL-A analytical ultracentrifuge. This article is dedicated to the memory of Phillip P. Smith.

SUPPORTING INFORMATION AVAILABLE

Figures showing series of elution profiles from the modified Hummel−Dreyer chromatography of LDH and αGDH and of LDH and ADH, and the corresponding plots of integrated αGDH or ADH peak areas versus [αGDH] or [ADH], for the conditions of [NADH]/[αGDH] = 0.0, 0.5 (plot only), and 2.0, and of [NADH]/[ADH] = 0.5. This material is available free of charge via the Internet at http://pubs.acs.org.

REFERENCES

1. Yong, H., Thomas, G. A., and Peticolas, W. L. (1993) Metabolite-modulated complex formation between α-glycerophosphate dehydrogenase and lactate dehydrogenase, *Biochemistry 32*, 11124−11131.
2. Wu, X., Gutfreund, H., Lakatos, S., and Chock, P. B. (1991) Substrate channeling in glycolysis: A phantom phenomenon, *Proc. Natl. Acad. Sci. U.S.A. 88*, 497−501.
3. Brooks, S. P. J., and Storey, K. B. (1991) Re-evaluation of the glycerol-3-phosphate dehydrogenase/L-lactate dehydrogenase enzyme system, *Biochem. J. 278*, 875−881.
4. Ovàdi, J. (1995) *Cell Architecture and Metabolic Channeling*, Molecular Biology Intelligence Unit, R. G. Landes Company, Austin, TX.
5. Svedruzic, Z. M. NADH Channeling Between Dehydrogenases: Enzyme Kinetics, Protein Interaction, and Molecular Modeling. Ph.D. Thesis, Oklahoma State University, Stillwater, OK, 2000.
6. *CRC Handbook of Chemistry and Physics* (1996) 78th ed., CRC Press, Boca Raton, FL.
7. Bergmeyer, H. U. (1974) *Methods of Enzymatic Analysis* (Bergmeyer, H. U., Ed.) 2nd ed., VCH, Weinheim, Germany.
8. Bergmeyer, H. U. (1983) *Methods of Enzymatic Analysis* (Bergmeyer, H. U., Ed.) 3rd ed., VCH, Weinheim, Germany.
9. Spivey, H. O., and Ovàdi, J. (1999) Substrate channeling, *Methods 19*, 306−321.
10. Demeler, B. (2003) *UltraScan 6.0—Ultracentrifugation Data Analysis Software*, University of Texas Health Science Center, San Antonio, TX (http://ultrascan.uthscsa.edu).
11. Gabellieri, E., and Strambini G. B. (1994) Conformational changes in proteins induced by dynamic associations: A tryptophan phosphorescence study, *Eur. J. Biochem. 221*, 77−85.
12. Srivastava, D. K., and Bernhard, S. A. (1986) Metabolic transfer via enzyme−enzyme complexes, *Science 234*, 1081−1086.
13. Rudolph, J., and Stubbe, J. (1995) Investigation of the mechanism of phosphoribosylamine transfer from glutamine phosphoribosylpyrophosphate amidotransferase to glycinamide ribonucleotide synthetase, *Biochemistry 34*, 2241−2250.

BI027244B